

Colour gamut boundary determination for digital imaging medium using two-variable high order polynomials

Haisong Xu, Yong Wang; State Key Laboratory of Modern Optical Instrumentation, Zhejiang University; Hangzhou, P. R. China

Abstract

In order to implement the cross-media gamut mapping in colour image reproduction, the gamut of each medium involved should be first determined. In this paper, a new model was proposed to fit the surface of gamut boundary by two-variable high order polynomials. A Neso cathode ray tube monitor was used to illustrate how to apply the model to determining the medium colour gamut boundary and to evaluate the accuracy of this method. The colour gamut boundary could be analytically expressed by six two-variable high order polynomial equations. The coefficients of each equation could be calculated by least square approximation using the data measured of the colours on the boundary. Several key issues about this method, including the determination accuracy, the optimal quantities of the colour samples and the appropriate orders, were discussed. The experimental data analysis showed that the colour gamut boundary of the CRT could be described accurately using six sets of two-variable high order polynomials, when the order was set to four and 5x5x6 colours on the gamut boundary were used for model training.

Introduction

Since colour gamut mapping was indispensable for cross-media colour management, the algorithms for accurate gamut boundary determination (GBD) of digital colour imaging devices had been discussed for many years, along with the improved requirement for high-fidelity colour reproduction.

Many methods^[1-4] were proposed and testified in the published literatures, which may be classified into two groups: the discrete methods and the analytical ones. For the discrete methods, for example, the classical LUT method and segment maxima gamut boundary description (SMGBD)^[5-7], a large number of colour samples on the gamut boundary were measured or calculated by device characterization models^[8], and then the gamut of the device was described by the collection of these discrete data. While for the analytical methods^[9], these special colours on the surface of the device colour gamut boundary were expressed as analytical equations. In comparison with the discrete method, there are many merits for the analytical model. With the analytical expression, the intersection point between a "mapping line" and the medium gamut boundary could be obtained more easily and efficiently, which could save considerable processing time for image reproduction application. In addition, the parameters needed for the analytical models could be much fewer than these of discrete methods for the same acceptable accuracy.

In this paper, a method was proposed to fit the surface of gamut boundary by two-variable high order polynomials (TVHOP). A Neso cathode ray tube (CRT) monitor was used in the experiment to implement this method, and the estimated accuracy was also presented.

Algorithm

The colour gamut of RGB imaging devices were limited by the three primary colour components, red, green and blue, which ranged from 0 to $2^N - 1$, where N denoted the bit depth of individual colour channel. The RGB data sets, of which one element was set as 0 or maximum, corresponded to the colours on the gamut boundary. Therefore, the surfaces corresponding to the six planes of the RGB cube space composed the device colour gamut boundary.

TVHOP model

Each surface of the colour gamut boundary can be expressed in the form of high order polynomials with the colorimetric coordinates a^* , b^* as the two independent variables and the lightness L^* as the dependent one. Firstly, appropriate number of colour samples on the gamut boundary were measured to obtain the accurate values of L^* , a^* and b^* . Then these colour samples were separated into six groups according to which plane they belonged to in the RGB space. The colour samples in the same group combined one surface of the colour gamut boundary. The curve fitting with high order polynomial regression was usually used in experimental data analysis. This principle can also be extended to fit the curve surface in the three-dimension dataset analysis. In the three dimension reference frame of L^* , a^* , b^* in this study, a curve surface could be defined as

$$L^* = \sum_{i=0}^{m-1} \sum_{j=0}^{n-1} p_{ij} (a^*)^i (b^*)^j, \quad (1)$$

where p_{ij} was the model coefficients, m and n were the order of the two independent variables respectively.

Model coefficient optimization

The coefficients, p_{ij} , of each curve surface could be calculated by least square approximation using the data measured of the colours on the boundary. The optimal coefficients, which minimized the difference between the L^* estimated and measured, should satisfied the following equations of

$$\frac{\partial S}{\partial p_{ij}} = 0, \quad ij = 0, 1, \dots, (m-1)(n-1) \quad (2)$$

$$S = \sum_{k=1}^g \left(\sum_{i=0}^{m-1} \sum_{j=0}^{n-1} p_{ij} (a^*)^i (b^*)^j - L^* \right)^2$$

where g was the number of sample colours on one plane of RGB cube. If \mathbf{P} represented the coefficient vector containing $(m-1) \times (n-1) + 1$ elements, $(m-1) \times (n-1) + 1$ equations in terms of matrix would be obtained from equation (2) as follows

$$\mathbf{AP} = \mathbf{B}, \quad (3)$$

where, the matrix \mathbf{A} and \mathbf{B} were calculated by the values of sample boundary colours in CIELAB colour space as following equations,

$$\mathbf{A} = \begin{pmatrix} (\varphi_{00}, \varphi_{00}) & (\varphi_{00}, \varphi_{01}) & \cdots & (\varphi_{00}, \varphi_{(m-1)(n-1)}) \\ (\varphi_{01}, \varphi_{00}) & (\varphi_{01}, \varphi_{01}) & \cdots & (\varphi_{01}, \varphi_{(m-1)(n-1)}) \\ \vdots & \vdots & \ddots & \vdots \\ (\varphi_{(m-1)(n-1)}, \varphi_{00}) & (\varphi_{(m-1)(n-1)}, \varphi_{01}) & \cdots & (\varphi_{(m-1)(n-1)}, \varphi_{(m-1)(n-1)}) \end{pmatrix}$$

$$\mathbf{P} = \begin{pmatrix} p_{00} \\ p_{01} \\ \vdots \\ p_{(m-1)(n-1)} \end{pmatrix}$$

$$\mathbf{B} = \begin{pmatrix} (\varphi_{00}, \bar{L}^*) \\ (\varphi_{01}, \bar{L}^*) \\ \vdots \\ (\varphi_{(m-1)(n-1)}, \bar{L}^*) \end{pmatrix}, (\varphi_{00}, \varphi_{00}) = \sum_{k=1}^g (a_k^*)^0 (b_k^*)^0 \bullet (a_k^*)^0 (b_k^*)^0$$

$$(\varphi_{00}, \varphi_{01}) = \sum_{k=1}^g (a_k^*)^0 (b_k^*)^0 \bullet (a_k^*)^0 (b_k^*)^1 \quad (4)$$

...

$$(\varphi_{00}, \bar{L}^*) = \sum_{k=1}^g (a_k^*)^0 (b_k^*)^0 \bullet \bar{L}_k^*$$

...

Then the model optimal coefficients were calculated by

$$\mathbf{P} = \mathbf{A}^{-1} \mathbf{B} \quad (5)$$

When six sets of coefficients for the surfaces of gamut were computed, the curve surfaces of colour gamut boundary could be analytically expressed by these six two-variable high order polynomials.

Edges of the gamut boundary

It was difficult to analytically express the twelve edges of the gamut boundary in a three-dimension colour space. However, the accurate description of these edges was very important for the gamut boundary determination, otherwise the analytical expression of the surfaces obtained in last section was not sufficient to determine the gamut boundary of imaging devices. A solution of the edge definition was to fit the projection of the edges on a^*b^* plane by use of an analytical two-dimension model, but it might result in additional modal error. Alternatively, the samples located on the edges could be taken as the supplement of the analytical expression of the gamut surfaces, as done in the experiments of this study.

The boundary polygons on constant hue plane

Since many cross-media gamut mapping algorithms were carried out on a given constant hue (h) plane, the calculation of the gamut boundary, which was composed by the intersection lines of the surfaces and this plane, should be firstly discussed here. For displays, which gamut boundary was consecutive, the boundary on the constant hue plane consisted of two or three segments to connect the peak white and black points. Each segment corresponded to one surface, which was intersected by the hue plane. In many cases, the number of segments was two. A case of $h = \pi / 4$ was shown in figure 1, where the boundary was simply represented as straight lines just for convenience, though not the case in nature.

The plane with constant hue, h , could be represented by

$$b^* = a^* \cdot \tan(h) \quad (6)$$

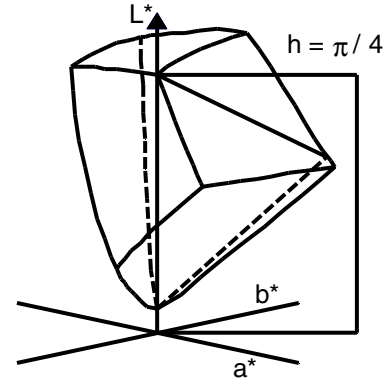


Figure 1. The gamut boundary on the plane of $h = \pi / 4$ in CIELAB colour space.

The horizontal coordinates of the constant h plane in figure 1 was defined as

$$C_{ab}^* = \sqrt{(a^*)^2 + (b^*)^2} \quad (7)$$

Combining equations (5), (6) and (7) to eliminate the variables a^* and b^* , the analytical expression of the boundary polygon on this plane was calculated as

$$\bar{L}^* = f(C_{ab}^*) \quad (8)$$

The function f depended on the given hue and the polynomials of the surface intersected, which should be firstly determined.

On the a^*b^* plane, it was determined which one of the six surfaces was intersected by the constant hue plane. The edges of the gamut boundary were projected onto a^*b^* plane, as shown in figure 2.

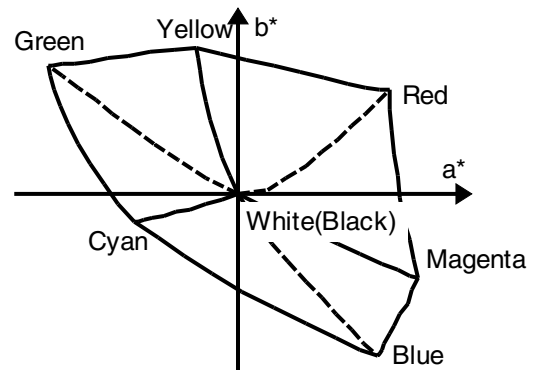


Figure 2. The projection of gamut boundary edges on the a^*b^* plane

For these edges not connected with the origin, whether the edges crossed with the straight line of constant hue could be judged by comparing the given hue and angles of the two lines from the $+a^*$ axis. In figure 3, for example, the lines of WR and WY connected the two ends of the edge and the origin respectively. If the given hue was between the two angles, α_{WR} and α_{WY} , the edge, YR, was determined to cross with the hue line, which also indicated that the surfaces containing this

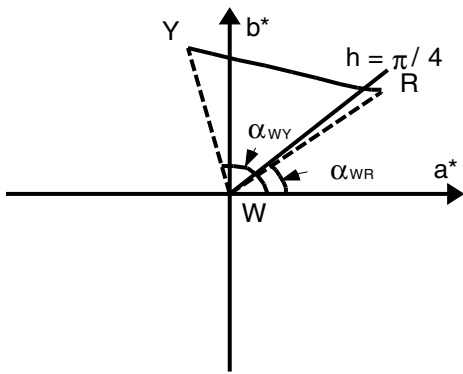


Figure 3. Intersection judgment method illustration for the edges not linked with the origin.

edge was intersected by the plane with the given hue. Then, the a^* , b^* values of the intersection point were linearly interpolated by the nearest sample points on the edge with the angle differences as weights. It was obvious that the a^* value of this point was surely be the upper limit of a^* of the boundary lines on the hue plane. The judgment method should be modified for those edges with the origin as one end. The angles for all points sampled on the edge except for the origin were calculated, and the maximum and minimum angles were found and compared with the hue angle. If the edges linked with origin crossed the given hue line, the number of segments was increased to three, which meant three surfaces were intersected by the plane with the given hue. This case was shown in figure 4, where the WR crossed the hue line of $h = \pi/6$. Three surfaces, KRMB ($G=0$), KGYR ($B=0$) and WYRM ($R=255$), were intersected by the plane of $h = \pi/6$, accordingly, three segments formed the whole line boundary on this hue plane. The intersection point should be calculated and taken as the start point of one segment, while as the end of the neighbor one. The boundary lines corresponding to figures 3 and 4 were plotted in $L^*C_{ab}^*$ plane as shown in figure 5.

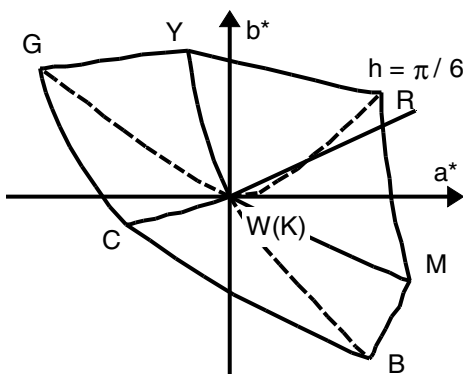


Figure 4. Intersection judgment method illustration for the edges linked with the origin

Experiments and results

The gamut boundary determination of a Neso FD570A CRT monitor, 15 inches, was performed using TVHOP

algorithm. The samples consisted of 10x10x6 RGB triplets on the gamut boundary by setting one of three channels to 0 or 255 in turn, while varying the other two channels in the collection of 0, 29, 57, 85, 114, 142, 170, 199, 227, and 255. The steps of the colour channel drive D/A values were different so that the samples were distributed more uniformly in CIELAB space. All the colours were measured using the telephotometer PR650 in a dark room. The display and measurement device were warmed up over one hour beforehand. Other conditions were consistent with the international electrotechnical commission standard, IEC 61966-3^[10].

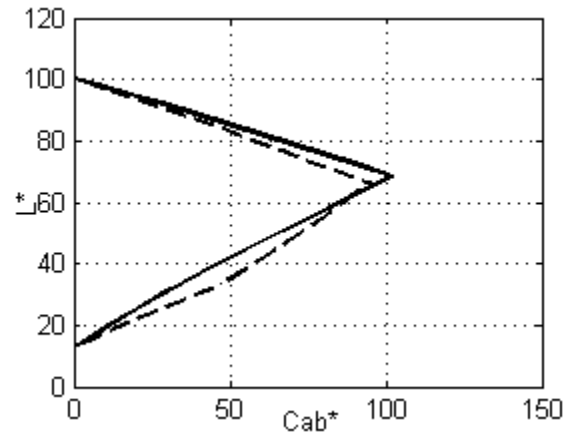


Figure 5. The boundary lines plotted in $L^*C_{ab}^*$ plane, the dashed lines were for the hue angle of $\pi/6$ and the solid ones for that of $\pi/4$.

Model accuracy

The gamut boundary determination accuracy of the TVHOP model was testified by the difference between the lightness measured and estimated according to equation (1).

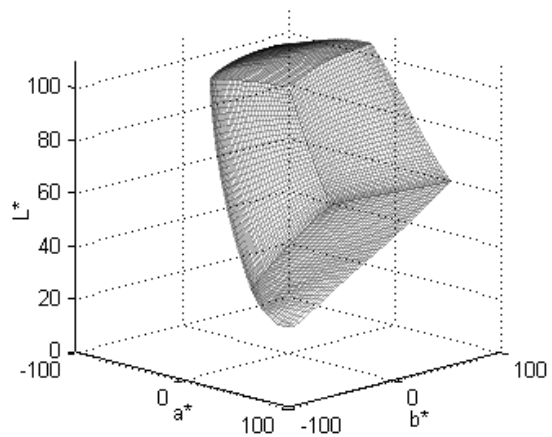


Figure 6. The gamut of Neso FD570A CRT determined by TVHOP model with the orders of six.

The tristimulus values measured of sample colours were transformed into CIELAB colorimetric parameters using the peak white as reference, X_n , Y_n and Z_n . The gamut determined by the TVHOP model was visualized in figure 6, in which the orders of the model, m and n , were set to six, and all sample data was used for model training. The statistics of the model

accuracy for each surface and all samples were summarized in table 1.

Table 1: The model accuracy, m=n=6, 10x10x6 sample colours for training and test.

Lightness difference	Mean	Std.	Min.	Max.
R=0	0.0621	0.0676	0.0014	0.4040
R=255	0.0362	0.0339	0.0001	0.1746
G=0	0.0576	0.0591	0.0003	0.4191
G=255	0.0330	0.0249	0.0014	0.1298
B=0	0.0638	0.0690	0.0007	0.3489
B=255	0.0512	0.0446	0.0005	0.2380
All colours	0.0506	0.0498	0.0001	0.4191

As can be seen in table 1, the TVHOP model was quite accurate with the mean lightness difference of 0.0506 and the maximum of 0.4191, when the orders were set to six and using 10x10x6 sample colours for training and test.

Optimal quantities of the samples and appropriate orders

Although the TVHOP model was great when the orders, m and n, were set to six and 10x10x6 colours on the gamut boundary were measured, the parameters of the model was increased to 6x6x6 and the measurement of these sample colours would cost too much time. Therefore, to find the optimal sampling methods and the appropriate orders for this model, several experiments were carried out, with the orders of the model were set to 2, 3, 4, 5 and 6, respectively. A sub-dataset including 5x5x6 samples, selected from the collection of RGB triplets used in the above experiment, was inserted into the model training, while a group of 10x10x6 colours was adopted to testify the determination accuracy of the model with different orders. The mean and maximum lightness differences of all test colours for each surface were plotted in figures 7 and 8.

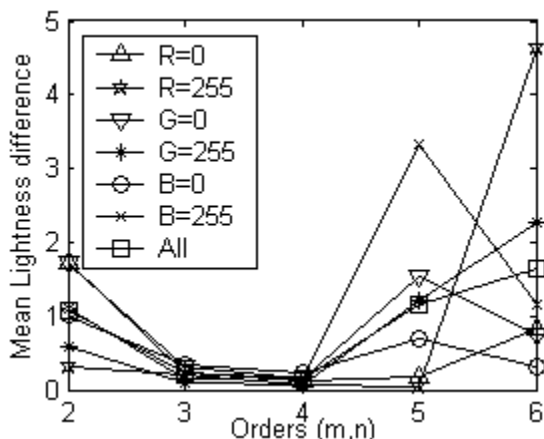


Figure 7. The mean lightness differences of TVHOP with different orders using 5x5x6 samples as training data while 10x10x6 colours for test.

The results showed that the orders should be set to 3 or 4, which was optimal for the model when 5x5x6 samples were used as training data. The mean and maximum lightness

differences of the four-order model for 10x10x6 test colours were 0.1392 and 1.9561, respectively. The model performance with the orders of three was slightly poor compared with that of the four-order model, but its accuracy, 0.2281 and 2.7553, was also acceptable.

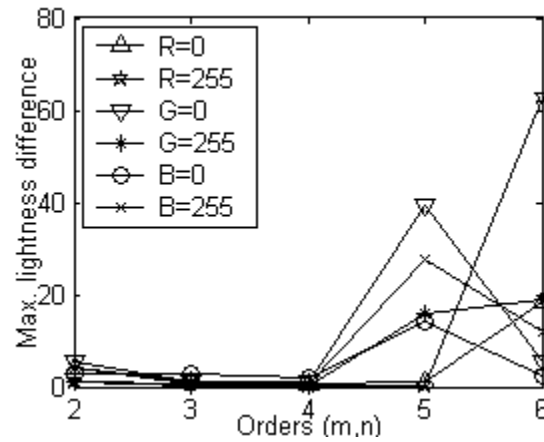


Figure 8. The maximum lightness differences of TVHOP with different orders using 5x5x6 samples as training data while 10x10x6 colours for test.

Figures 9 to 12 illustrated the comparison of the boundary lines on the planes of four constant hues, $\pi/4$, $(3/4)\pi$, $(5/4)\pi$ and $(7/4)\pi$, calculated by the models with the orders of 4 and 6, respectively, in which the former employed 5x5x6 sample colours in the polynomial fitting, while the latter was trained with 10x10x6 samples. In the figures, the solid lines corresponded to the former model, which was considered as the reference to evaluate the accuracy of the latter model as represented in dashed lines.

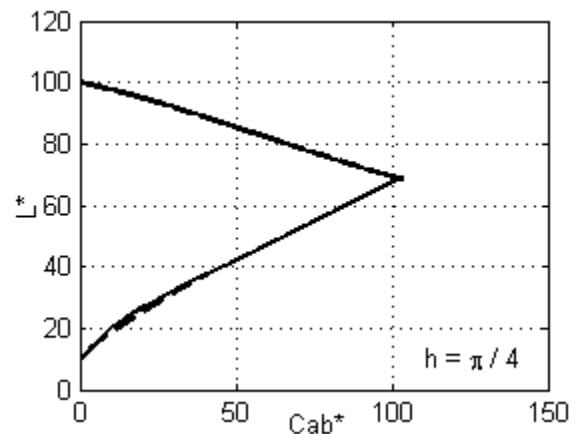


Figure 9. Comparison between the boundary lines calculated by the model with different orders of 4 and 6 on the constant hue plane of $h = \pi/4$.

These figures indicated that the model with the orders of four and 5x5x6 training samples was quite accurate for the boundary polygon calculation on the constant hue plane. The segments with the lightness lower than 40 showed some small estimation errors on the planes of $h = \pi/4$ or $(3/4)\pi$, as in figures 9 and 10, while the other parts of the boundaries were almost identical in all figures. The experimental results implied that the accuracy of the four-order model might be improved by

means of increasing the sample colours with low lightness on the R=0, G=0 and B=0 surfaces.

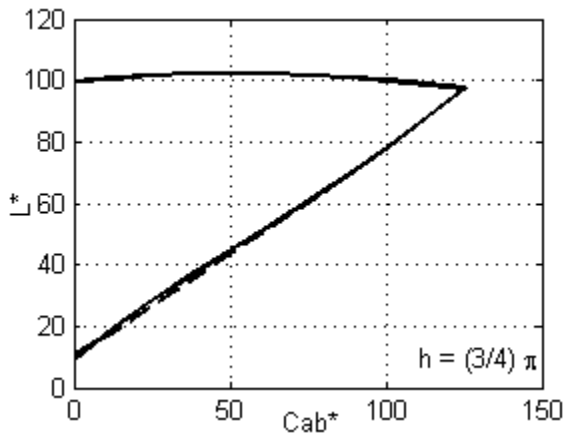


Figure 10. Comparison between the boundary lines calculated by the model with different orders of 4 and 6 on the constant hue plane of $h = (3/4)\pi$.

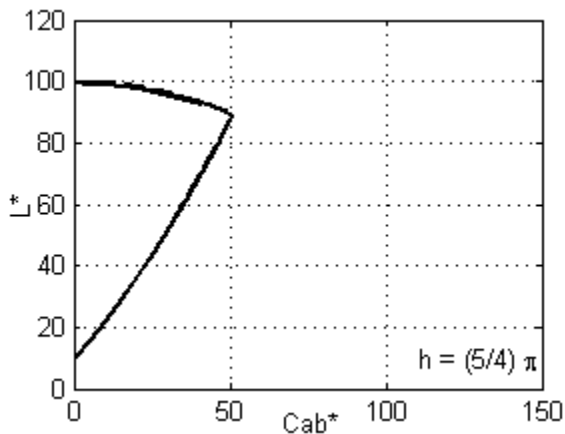


Figure 11. Comparison between the boundary lines calculated by the model with different orders of 4 and 6 on the constant hue plane of $h = (5/4)\pi$.

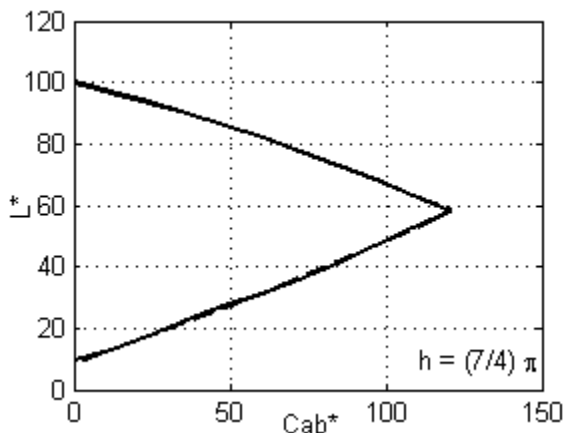


Figure 12. Comparison between the boundary lines calculated by the model with different orders of 4 and 6 on the constant hue plane of $h = (7/4)\pi$.

Conclusions

Based on the optimization with least square estimation method, a new TVHOP model, consisting of six sets of two-variable high order polynomials was proposed for analytical expressing the gamut boundary of colour imaging devices. With this new model, the boundary polygon was separated into two or three segments, which were described by polynomials as equation (8) with different parameters, depending on the given hue and the intersected surface expressions. Then, the intersection point between any “mapping line” and the medium gamut boundary on the constant hue plane could be deduced rapidly and accurately.

The model optimization method and the boundary polygon calculation on the given hue plane were discussed in details. In the model accuracy test experiment on a CRT monitor, when 10x10x6 samples were used for training, the mean and maximum errors of six-order polynomials reached 0.0506 and 0.4191, respectively. However, so many samples and high orders were not practicable because of too much time cost and low algorithm efficiency. A reasonable number of samples, 5x5x6, were investigated for several types of polynomial with the orders ranged from two to six. The experimental results showed that the model with three- or four-order polynomials were accurate for the colours on all gamut boundary surfaces, in which the latter was considered to be the optimal choice with a relatively better performance in this study.

Finally, the boundary polygons on the four constant hue planes, $\pi/4$, $(3/4)\pi$, $(5/4)\pi$ and $(7/4)\pi$, were compared, using the same model with two different sets of training samples and orders. The boundary determined by the six-order model with 10x10x6 training samples taken as the reference, representing the nature of the gamut to some degree, the four-order model, optimized by 5x5x6 sample data, performed well.

Acknowledgement

This research work was supported by the National Nature Science Foundation of China under Grant No. 60578011.

References

- [1] G. Braun, M. Fairchild, Techniques for Gamut Surface Definition and Visualization, Proc. 5th Col. Imaging Conference, pg. 147 (1997).
- [2] M. Inui, Fast Algorithm for Computing Color gamuts, Col. Res. Appl., 18, 341 (1993)
- [3] J. Pujol, M. Verdú, P. Capilla, Estimation of Device Gamut of a Digital Camera in Raw Performance Using Optimal Color-Stimuli, Proc. PICS, pg. 530, (2003)
- [4] P. Pellegri, R. Schettini, Gamut Boundary Determination for a Colour Printer using the Face Triangulation Method, Proc. SPIE 5008, pg. 542 (2003).
- [5] J. Morovič, M. Luo, Calculating Medium and Image Gamut Boundaries for Gamut Mapping, Col. Res. Appl., 25, 394 (2000)
- [6] J. Morovič, P. Morovič, Determining Colour Gamuts of Digital Cameras and Scanners, Col. Res. Appl., 28, 59 (2000)
- [7] J. Morovič, P. Sun, P. Morovič, The Gamuts of Input and Output Colour imaging media, Proc. SPIE 4300, pg. 114. (2001).
- [8] Y. Wang, H. Xu, Determination of CRT Color Gamut Boundaries in Perceptual Color Space, Proc. SPIE 5637, pg. 332. (2005).
- [9] Q. Huang, D. Zhao, Gamut Boundaries Expressed with Zernike Polynomials, Proc. SPIE 4922, pg 149 (2002).
- [10] IEC 61966-6, Colour Measurement and Management in Multimedia Systems and Equipment – Part 3: Equipment Using Cathode Ray Tubes, Committee Draft, (1998).

Author Biography

Haisong Xu received his PhD in optical engineering from Zhejiang University (1993). From 1999 to 2001, he was a postdoctoral research fellow at the Department of Information and Image Sciences in Chiba University of Japan. Now he is a professor in the State Key

Laboratory of Modern Optical Instrumentation at Zhejiang University in China. His current research interests include colour vision, colour imaging, colorimetry, photometry, and etc.

Yong Wang is a PhD student in Zhejiang University. His research direction was colour management system.